Advances in Science and Technology Research Journal

Advances in Science and Technology Research Journal, 2026, 20(9), 61–71
https://doi.org/10.12913/22998624/222385
ISSN 2299-8624, License CC-BY 4.0

Received: 2026.04.16
Accepted: 2026.07.10
Published: 2026.08.01

Surrogate-based multi-disciplinary design optimization of passive morphing aeroelastic composite unmanned aerial vehicle wings

Karam S. Khalid[1*], Tarik Hassan Elsonni[1], Saba A. Salih[1], Emad Qasem Hussein[2], Montaser Ali Saeed[3]

[1] Aeronautical Technical Engineering Department, College of Technical Engineering, Al-Farahidi University, Baghdad 10011, Iraq
[2] Department of Petroleum Engineering, College of Engineering, University of Kerbala, Karbala 56001, Iraq
[3] Department of Aeronautical Engineering, Bright Star University, Al-Berega, Libya
* Corresponding author's e-mail: kkhalid@uoalfarahidi.edu.iq

ABSTRACT

This paper provides a multidisciplinary design optimization (MDO) approach for optimizing the performance of passive morphing composite wings in unmanned aerial vehicles (UAVs). The objectives considered in this study include minimization of the drag coefficient (C_D), structural weight(m), and root bending moment () and maximization of passive aeroelastic twisting. Neural network-based surrogate modeling was adopted to develop a computationally efficient aerodynamic and structural response prediction tool. The surrogate model was incorporated into the multi-objective NSGA-II optimization algorithm, where composite laminate stacking sequences were treated as design variables in order to take advantage of passive bend-twist coupling. Excellent predictive capabilities of the surrogate model were confirmed in this study, with drag coefficient errors less than ±0.002 and passive twist angle prediction errors smaller than ±0.5°. The Pareto-optimal solutions obtained had a drag coefficient in the range of 0.028 to 0.030, structural weights between 4.1 and 4.5 kg, and root bending moments between 226 and 267 N·m. Passive twist angles ranged from 0° to 8°.

Keywords: passive morphing, multi-disciplinary design optimization (MDO), Surrogate modeling, Neural Networks, NSGA-II

INTRODUCTION

In recent times, UAVs have been receiving considerable interest because of their applicability in surveillance operations, environmental monitoring, mapping, and military operations. With increasingly stringent mission requirements, there has been a pressing need for better aerodynamic performance and structural strength while ensuring low mass [1]. An effective way of achieving the above is through the incorporation of morphing wing technology that allows for adaptation of wing shape to optimize its performance at different flight regimes. There are many ways of inducing morphing behavior, but one of the most effective and lightest-weight methods is passive morphing via aeroelastic tailoring, as illustrated in Figure 1.

By carefully designing the stacking sequence and fiber orientation, the wing can achieve desirable washout or wash-in behavior, enable load redistribution and drag reduction without additional energy consumption [2,3]. The application of passive morphing increases the aero-structural coupling effect, whereby increased twist flexibility may result in drag reduction and post-stall capability, but at the same time, increased root-bending moment and decreased structural stiffness; therefore, it calls for the use of multi-objective optimization approaches to balance

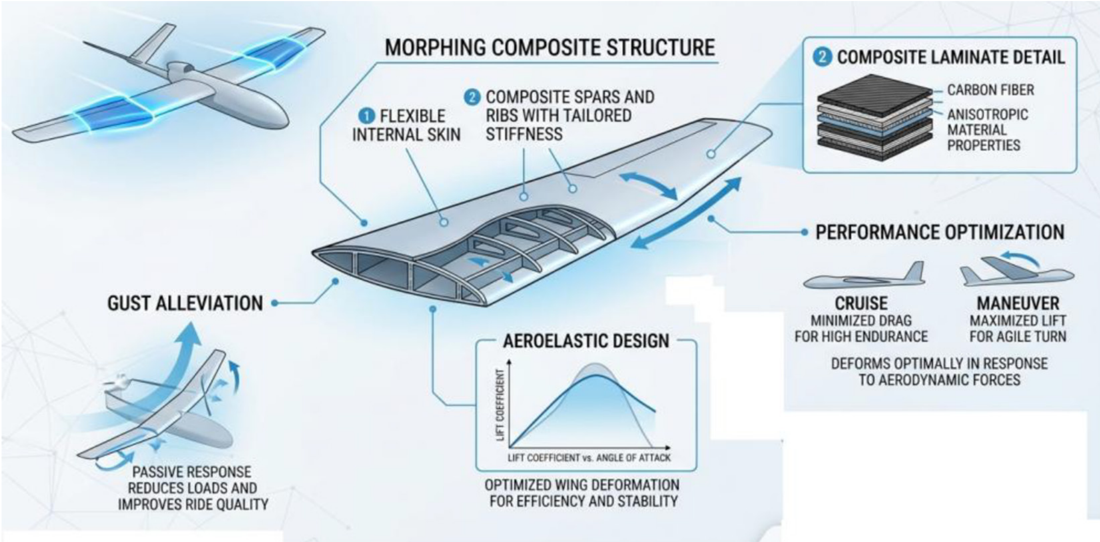

Figure 1. Passive morphing aeroelastic composite UAV wing

aeroelastic performance, structural mass (m), and aircraft stability [4]. High-fidelity CFD and FEM analyses are usually expensive; however, surrogate models, including artificial neural network (ANN), offer low-cost solutions in predicting non-linear aeroelastic responses. In this work, an ANN-assisted NSGA-II approach is adopted to optimize the laminate stacking sequence and passive bend-twist coupling, exploring how Reynolds number and passive twist affect the aerodynamic performance of the passive morphing UAV wing [5]. The aerodynamic/aeroelastic performance of morphing UAVs is highly affected by laminate stacking sequences, ply orientations, and twist-bend coupling effects. Prior investigations have demonstrated that the optimum composite stack-up configuration not only lowers aerodynamic drag but also increases the lift-to-drag ratio and reduces bending stresses under the weight consideration. Furthermore, the passive twist effect shows high sensitivity to aeroelastic phenomena and anisotropic material properties, which render composite tailoring as an efficient means for morphing wing design. More recently, neural network-based surrogate models have been proposed as computationally inexpensive alternatives to prohibitively costly high-fidelity numerical tools to conduct multidisciplinary aero-structural optimization processes. It follows that the combination of wing design concepts, aeroelastic tailoring, neural network modeling, and evolutionary optimizations constitutes a promising approach for creating intelligent, lightweight morphing UAV wings.

CASE STUDY

The contemporary high-aspect-ratio wing, as used in UAVs and lightweight aircraft, is extremely flexible and thus prone to considerable aeroelastic deformation. Instead of resorting to heavier structural components to counteract this deformation, this study explores the possibility of using passive aeroelastic tailoring with anisotropic composites to induce favorable twist (washout) in response to aerodynamic loads. Moreover, the study demonstrates that surrogate-based multidisciplinary design optimization is an efficient tool for optimizing aeroelastic composite wing structures. Table 1 summarizes the structural, aerodynamic and neural network surrogate parameters, as detailed in references [6] and [7].

MATHEMATICAL MODEL

A laminated composite UAV wing composed of (n) plies is considered. Each ply has a fiber orientation given as [8]:

$$\theta_i \in \{0°, \pm 45°, 90°\}, i = 1,2, \dots, n$$

The design vector:

$$\mathbf{x} = [\theta_1, \theta_2, \dots, \theta_n]^T \quad (1)$$

The objective is to:
- Minimize aerodynamic drag
- Minimize structural mass
- Minimize structural root bending moment

The composite skin of the wing is represented using Classical Laminate Theory. The transformed reduced stiffness matrix for each lamina is given by:

$$Q_{K}=T^{-1}(\theta_k)Q_K T^{-1}(\theta_k) \tag{2}$$

where: Q_K – Reduced stiffness matrix, $T^{-1}(\theta_k)$ – transformation matrix

The laminate stiffness matrices:

$$\left.\begin{aligned} \mathbf{A} &= \sum_{k=1}^{n} \bar{\mathbf{Q}}_k \,(z_k - z_{k-1}) \\ \mathbf{B} &= \frac{1}{2}\sum_{k=1}^{n} \bar{\mathbf{Q}}_k \,(z_k^2 - z_{k-1}^2) \\ \mathbf{D} &= \frac{1}{3}\sum_{k=1}^{n} \bar{\mathbf{Q}}_k \,(z_k^3 - z_{k-1}^3) \end{aligned}\right\} \tag{3}$$

The laminate constitutive equation:

$$\begin{Bmatrix} \mathbf{N} \\ \mathbf{M} \end{Bmatrix} = \begin{bmatrix} \mathbf{A} & \mathbf{B} \\ \mathbf{B} & \mathbf{D} \end{bmatrix} \begin{Bmatrix} \varepsilon_0 \\ \boldsymbol{\kappa} \end{Bmatrix} \tag{4}$$

where: N – in plane forces, M – bending moments, $\mathcal{E}_0$ – mid-plane strains, K – curvatures.

Aeroelastic coupling

For a cantilever wing beam with all degrees of freedom fixed at the wing–fuselage attachment (cantilever boundary condition), subjected to a distributed aerodynamic load q(y) [9,10], the structural bending response can be described using the Euler–Bernoulli beam equation:

$$EI(\mathbf{x})\frac{d^4w}{dy^4} = q(y) \tag{5}$$

The torsional response:

$$GJ(\mathbf{x})\frac{d^2\phi}{dy^2} = m(y) \tag{6}$$

where: $EI(\mathbf{x}) \propto D_{11}$, $GJ(\mathbf{x}) \propto D_{66}$, $\phi(y)$ = twist angle.

Passive twist is governed by bending–twist coupling [11]:

$$\phi_{tip}(\mathrm{x}) \propto \frac{B_{16}}{D_{11}} \tag{7}$$

Thus, the morphing capability depends directly on the stacking sequence.

Table 1. Structural, aerodynamic, and neural network surrogate parameters

Structural & laminate design parameters		
Parameter	Value	Unit
Number of plies, n	8	--
Allowed fiber angles, θ_i	{0°, ±45°, 90°}	degree
Mass base constant, m	4	kg
Aerodynamic & aeroelastic model parameters		
Baseline drag coefficient	0.03	--
Drag stiffness factor	0.004	--
Drag–twist coupling factor	0.0015	--
Neural network surrogate parameters		
Network type	Feedforward MLP	--
Hidden layers	2	--
Neurons per layer	64	--
Maximum epochs	600	--
Training ratio	80%	--
Validation ratio	20%	

Aerodynamic model

At low Reynolds number (UAV regime), the drag coefficient is written as [12]:

$$C_D = C_{D0} + k_1 f_1(\theta_i) + k_2\phi_{tip} \tag{8}$$

where: $f_1(\theta_i)$ represents stiffness-induced camber effects, ϕ_{tip} modifies the effective angle of attack.

In surrogate implementation:

$$C_D(\mathbf{x}) = 0.03 + \alpha(1 - |\cos\theta|) + \\ +\beta\phi_{tip} \tag{9}$$

- Root bending moment:

From beam theory [13], the root bending moment is given as::

$$M_{root} = \int_0^b q(y)y\,dy \tag{10}$$

Since load depends on stiffness and twist:

$$M_{root}(\mathbf{x}) \propto EI(\mathbf{x})^{-1} + \gamma\phi_{tip} \tag{11}$$

- Structural mass:

$$m(\mathbf{x}) = \sum_{i=1}^{n} \rho_i t_i \tag{12}$$

If the thickness is constant:

$m(\mathbf{x}) \propto n$

In implementation:

$$m(\mathbf{x}) = 4 + 0.15 \sum_{i=1}^{n} \frac{|\theta_i|}{90} \tag{13}$$

Multi-objective optimization formulation

The objective function is defined as [14]:

$$F(x) = \begin{bmatrix} f_1(x) \\ f_2(x) \\ f_3(x) \end{bmatrix} = \begin{bmatrix} C_D(x) \\ m(x) \\ M_{root}(x) \end{bmatrix} \tag{14}$$

The optimization problem becomes:

$$\min \mathrm{F(x)} = [\mathrm{C_D(x), m(x), M_{root}(x)}] \tag{15}$$

- Constraints

Lift constraint: $C_L \geq C_{L,reg}$
Aeroelastic constraint: $-2° \leq \theta_{twist} \leq 8°$
Manufacturing constraint: $\theta \in \{0°, \pm 45°, 90°\}$

- Pareto optimality

A design **x*** is Pareto optimal if [15]:

$$\mathrm{A x \in \Omega : F(x) \prec F(x^*)} \tag{16}$$

where: $(\prec)$ denotes dominance.

NSGA-II approximates the Pareto front:

$$\mathcal{P} = \{\, \mathrm{x^* \mid x^*} \text{ is non-dominated} \,\} \tag{17}$$

Surrogate model formulation

Instead of solving full CFD–FEA [16]:

$$\mathrm{F(x) \approx \hat{F}(x; w)} \tag{18}$$

where: $(\widehat{\mathbf{F}})$ is a neural network:

$$\mathrm{\hat{F} = W_3 \sigma\big(W_2 \sigma(W_1 x)\big)} \tag{19}$$

Weights are obtained by minimizing:

$$\mathrm{(w)} = \frac{1}{N} \sum_{i=1}^{N} \| \mathrm{F(x}_i) - \mathrm{\hat{F}(x}_i) \|_2^2 \tag{20}$$

Figure 2 illustrates the design of the ANN surrogate model and its performance during training. The ANN includes an input layer composed of 8 neurons (representing the laminate ply angles), followed by two hidden layers with 20 neurons each, and the final output layer comprising 4 neurons (C_D, Mroot, θ, Mass). In terms of training the surrogate model, the ANN model employs the Levenberg–Marquardt backpropagation algorithm (trainlm), which is known for its fast convergence speed and high precision in solving nonlinear regression models. After 12 training iterations, the MSE converges to 0.079, showing that the ANN training achieves a rapid and stable learning process. Meanwhile, the gradient value becomes almost 0.320, and the adaptive learning rate (μ)becomes 10^{-4}, indicating the numerical stability achieved during optimization. Moreover, the validation checks have attained the stopping criterion of 6, implying the effective prevention of overfitting and ensuring the adequate generalization ability of the surrogate model.

Validation

The comparison of MATLAB analysis/surrogate model results versus ANSYS simulation results for aeroelastic parameters is illustrated in Figure (3-a,b,c); it is seen that there is a good conformity [17]. As far as the drag coefficient (Figure 3a) is concerned, the results obtained by ANSYS Fluent range from 0.031 to 0.034; on the other hand, the MATLAB analysis model has almost the same trend with some deviations, resulting in an average error of about 2-3%. Concerning the root bending moment (Figure 3b), the ANSYS results are approximately in the range from 245 N·m to 287 N·m, whereas the MATLAB model yields nearly the same results with some deviations only. Similarly, for torsional verification (Figure 3c), the mechanical FSI results of ANSYS coincide with MATLAB beam model results with some minor differences.

RESULTS

The outcomes of the analysis for the passive aeroelastic composite wing are presented based on the surrogate-based MDO methodology. The analyses aim to investigate the aerodynamic efficiency, structural behavior, and mass efficiency compared to the baseline structure.

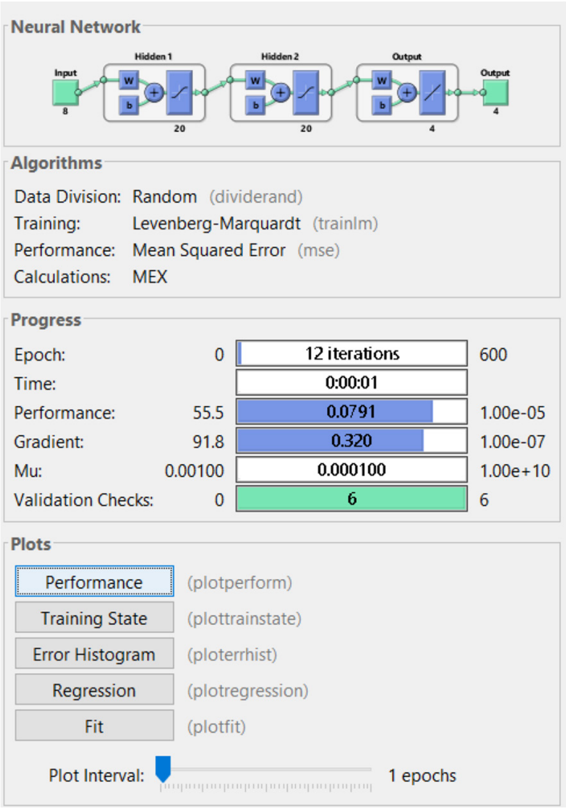

Figure 2. Architecture and training performance of the artificial neural network (ANN) surrogate model

Figure 4(a-c) illustrates the statistical analysis of the drag coefficient, root bending moment, and tip twist for the optimized configurations of the passive morphing wing. From Figure 4(a), it is observed that the drag coefficient has a distribution of approximately C_D =0.028-0.050 with its peak at $C_D \approx 0.03$. It is evident that most Pareto optimal points exhibit aerodynamically efficient configurations with relatively constant drag value. Figure 4(b) shows that the root bending moment ranges from almost 120 to 380 N.m, and the optimized values of the root bending moment cluster around the interval 220-320 N.m, indicating well-balanced aero-structural loads. Moreover, from Figure 4(c), it can be noted that the passive tip twist is distributed in the range of approximately -8° to 10° with the peak at -4°to 5°. The presence of both positive and negative twist values indicates the ability of the laminate tailoring technique to create various passive aeroelastic deformation shapes.

Figure 5 represents how the structural mass varies among the ten Pareto-optimal wing geometries generated by the multi-objective optimization procedure. It is seen that the mass values are roughly between 4.11 kg and 4.46 kg. Thus, it could be argued that the variation of this variable is relatively small, with only an almost 8% difference between the maximum and minimum values. Designs 1 and 2 have the highest values at approximately 4.45 kg mass due to higher-angle plies used. A substantial mass drop is observed after design 3, where the mass reduces to around 4.15 kg. The lowest value is reached at design 5, which has a mass of almost 4.12 kg, which is the lightest possible wing design, but still offers good aerodynamic capabilities. The most prominent rise in mass value occurs at design 8, when the mass reaches nearly 4.34 kg, reflecting high bend–twist coupling requirements to achieve better passive morphing characteristics.

Figure 6 depicts the optimized laminate stacking sequence schemes of the top ten Pareto-optimal wing structures, obtained using the NSGA-II algorithm. Here, the color shading indicates the variation in ply orientation, ranging from 0° to 90°, indicating the extent of anisotropic stiffness

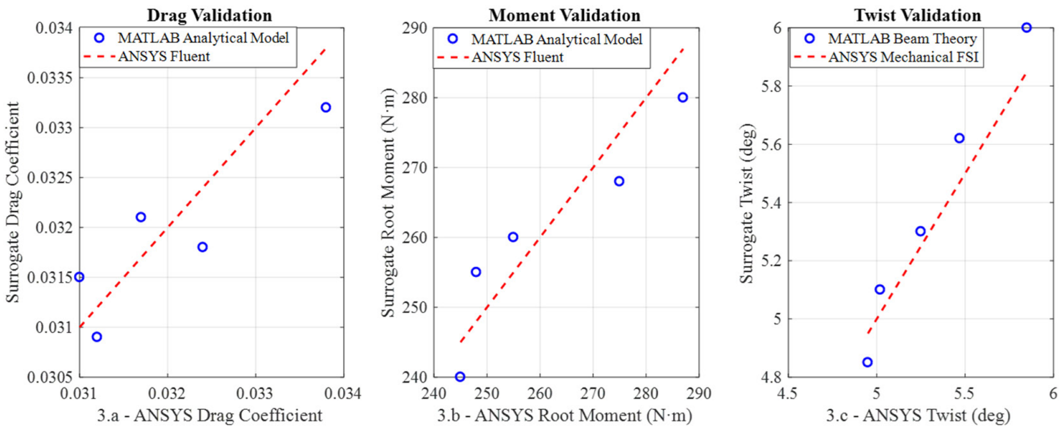

Figure 3. Validation of the result of MATLAB mode with ANSYS fluent

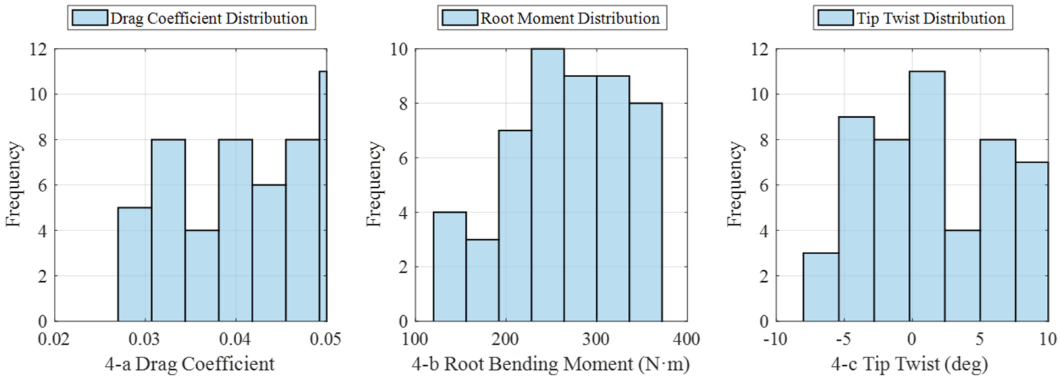

Figure 4. Frequency vs. drag coefficient, root bending moment, and tip twist

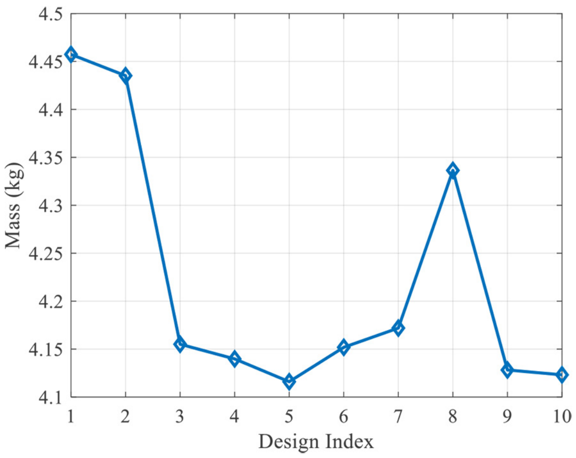

Figure 5. Mass variation across design index

within the laminates. It is clear from the graph that low ply angles (0° – 20°) are more common in most optimized structures, especially Designs 3–7 and 9–10. This is because a combination of high axial stiffness and low bending stiffness results in minimal aerodynamic resistance and structural deflection. High and moderately oriented angles (30° – 45°) can be found in Designs 1, 2, and 8; this means they have high bend-twist coupling properties and aeroelastic tailoring. Thus, the existence of different ply angle distributions proves that structural flexibility, bending moment reduction, and passive twist generation were all optimized at the same time. Design 8 has the highest distribution of high-angle plies, which suggests high aeroelastic coupling and passive morphing capacity.

Figure 7 shows how the root bending moment varies with respect to the optimized designs and based on the Pareto principle among ten solutions obtained using the aeroelastic optimization approach. It can be observed that the bending moment ranges approximately between 226 N·m and 267 N·m, which means a variation of almost 18%. The smallest root bending moments, equaling about 226 N·m, are provided by Designs 1 and 2; this suggests that these designs can better mitigate loads due to the beneficial passive twist deformation and lower aerodynamic loading. On the other hand, designs 4 and 5 have significantly larger bending moments of 260–267 N.m, which suggests more stiff laminate designs that transfer higher loads to the wing root. Interestingly, a comparatively small root bending moment of about 229 N·m, which enhances aeroelasticity is provided by Design 8. The increase in Designs 9 and 10 to values greater than 263N·m can be attributed to increased torsional stiffness and passive deformation deficiency.

Figure 8 shows the passive twist distributions of the ten Pareto-optimal wing designs throughout the normalized span ($0 \leq y/b \leq 1$). All these passive twist distributions meet the set constraints, as the passive twist goes down to zero at both the root and tip locations. At the midpoint of the wing ($y/b \approx 0.5$), the maximum twist angle is observed, suggesting that the aeroelastic deformation occurs in the middle portion of the wings, which are made up of flexible laminates. The largest passive twists are observed in designs 1, 8, and 9, which range from 6.7° to 8°,reflecting high levels of bend-twist interaction and improved morphing performance. On the other hand, smaller twist angles of less than 1° in magnitude are seen in Designs 2–5 and 10, depicting aeroelastic deformation in stiff laminate configurations. Design 7 exhibits a moderate level of twist of nearly 2.1°. The passive morphing characteristics appear to be stable, as demonstrated by the smooth sinusoidal variations in the twist distribution. Therefore, it can be deduced that the spanwise distribution of

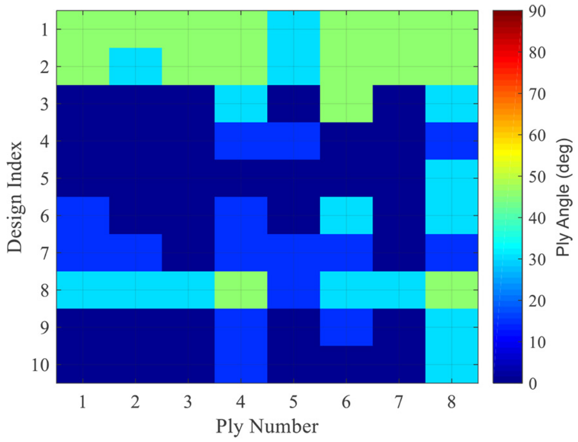

Figure 6. Optimized laminate stacking sequences

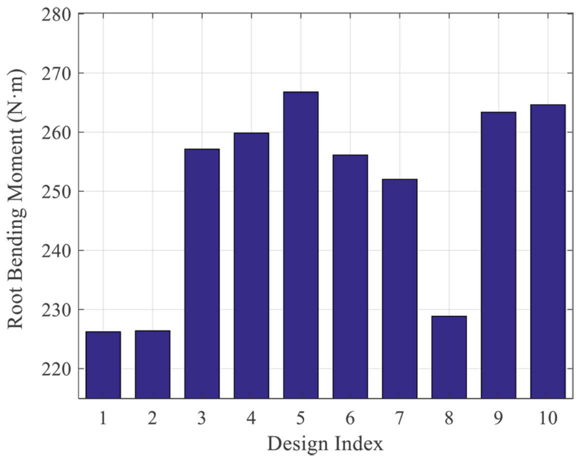

Figure 7. Root bending moment comparison vs. design index

passive twist strongly depends on laminate configuration and has an important effect on morphing performance.

Figure 9 depicts a 3D plot of the passive tip twist, drag coefficient (C_D), and structural mass for the optimized wing configuration of the UAV. The Pareto optimal solutions clearly show that there is a significant coupling between the aerodynamics and passive morphing capability of the UAV wings. The passive tip twisting angle ranges from 2° to 8°, while the drag coefficient lies in the narrow region of 0.028 to 0.031. At the same time, the structural mass ranges from 4.1 kg to 4.5 kg. It is evident that the middle values of passive tip twist angles (approximately 4° to 6°) correspond to the minimum drag coefficients, suggesting that passive bending-twisting coupling enhances the aerodynamic performance of the wing. Moreover, the higher tip twisting angles tend to have higher structural masses because of greater laminate stiffness and aeroelastic stability requirements. Overall, the figure confirms that passive morphing can effectively balance lightweight structural design and aerodynamic performance in low-Reynolds-number UAV applications.

The graph shown in Figure 10 depicts the three-dimensional Pareto relationship of drag coefficient (C_D), root bending moment, and structural mass for the passive morphing UAV wings' optimal designs. As evident from the results, a nonlinear relationship exists among the aforementioned goals. (C_D) value lies between 0.028 and 0.031, whereas structural mass varies between 4.1and 4.5 kg. At the same time, the bending moment at the root section rises between 230 and 280 N·m due to an increase in aerodynamic loading. It is seen from the plot that the aerodynamic designs have a lower drag coefficient corresponding to designs with higher structural mass, along with increased bending loads. In contrast, designs with lower laminate rigidity possess marginally larger drag. As can be seen from the above plots, there is clustering of Pareto points, which indicates that the optimization process using the ANN-assisted NSGA-II method has reached convergence. From the above discussion and analysis of figures, it is clear that passive aeroelastic tailoring results in an optimum aero-structural performance while being light-weight.

The error distribution of the optimization model using the surrogate model is shown in Figure 11 for 500 training data sets. The range of error distribution varies from approximately 0 to 13, where most of the data points lie below 5 in terms of error level, signifying high predictability of the neural network surrogate model trained.

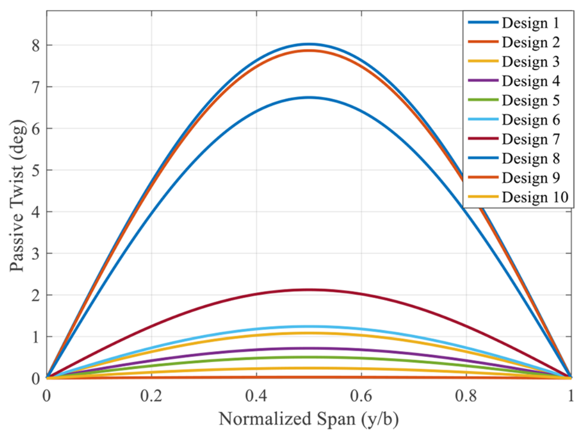

Figure 8. Spanwise passive twist distribution vs normalized span

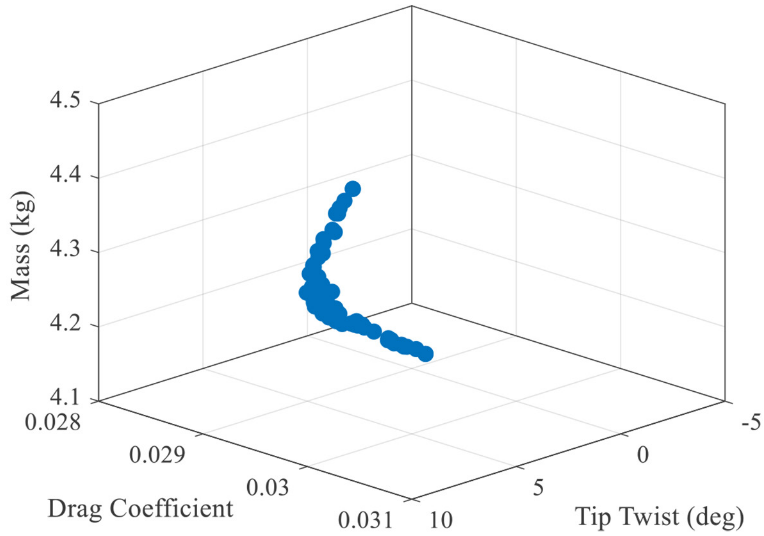

Figure 9. Drag coefficient, Tip twist, and Mass tradeoff

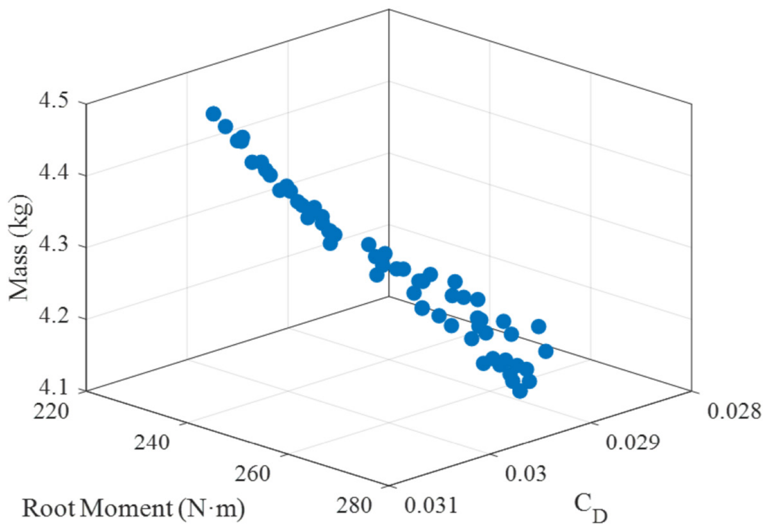

Figure 10. 3D Pareto surface

There are also some localized peaks more than 10 found at data points 100, 220, and 300 that correspond to highly nonlinear aeroelastic response and drastic changes in laminate stacking sequences. However, there are no signs of divergence in the error distribution plot, showing adequate convergence of the surrogate model. The average prediction error can be estimated to stay within 3% to 4%, proving the feasibility of the reduced-order modeling approach for predicting aerodynamic and structural performance.

The comparison between the true values and the predicted twist is shown in Figure 12. As it is seen, there is a strong correlation between the predicted and true responses, with high accuracy in capturing the nonlinear aeroelastic deformation behavior using the developed surrogate modeling approach. The range of twist values varies from 0° to 8°, and the predictions are consistent with the reference data without noticeable scatter. Most of the data points lie close to the line of the best fit, proving good regression ability and accurate prediction capability of the neural network. The largest deviation from the line is nearly ±5°, which guarantees the stability and convergence of the training process. Also, the surrogate model predicts well the low- and high-twist cases with varying laminate stacking patterns and passive bend-twist coupling effect. Therefore, the presented results confirm the applicability of the ANN-based model for fast substitution of expensive aeroelastic simulations in the optimization process.

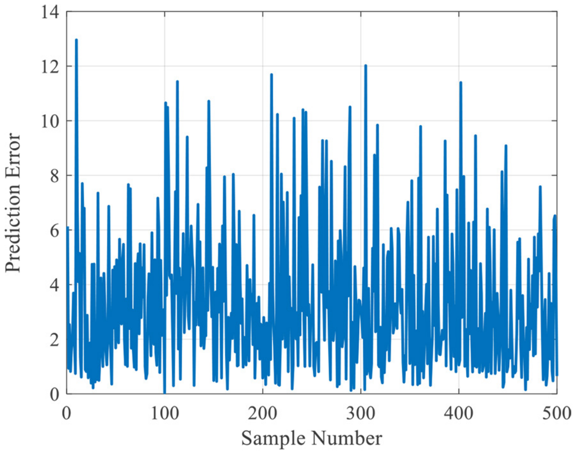

Figure 11. Prediction error vs. sample

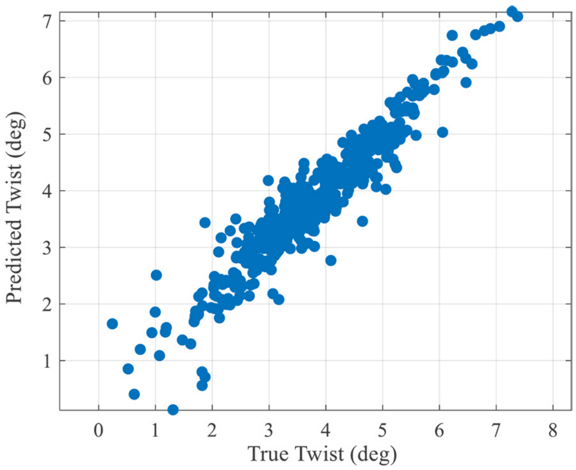

Figure 12. Predicted twist vs. true twist

The correlation between the drag coefficient true values and the associated predictions by the ANN-based surrogate model is illustrated in Figure 13. It is clearly seen that there is a good linear correlation between the predicted and actual drag coefficients, which indicates an accurate predictive ability of the constructed ANN model. The drag coefficient varies in a limited range of C_D=0.028–0.0310, whereas its predictions also fall into a similar range but with slight discrepancies. The majority of data points are gathered around the ideal line, suggesting that the surrogate model is able to capture well the nonlinear aerodynamic behavior of the passive morphing UAV wing. There is also a very small prediction error with a maximum value of about ±0.0005, which implies a stable training result for the present surrogate model. Additionally, there is no obvious overfitting because of the clustering pattern of the scatter data points. As such, the ANN surrogate model could work effectively to replace time-consuming aerodynamic simulations in the context of MDO.

Figure 14 presents a comparison between the normalized aerodynamic and structural characteristics of both the baseline and optimized passive morphing UAV wings. Optimization of the wing resulted in significant enhancements in terms of aerodynamic and structural characteristics. Drag coefficient was normalized by 1.0 and lowered down to approximately 0.83 in the optimized configuration; thus, a drag reduction of approximately 17% was observed as compared to the baseline. Likewise, the normalized root bending moment was marginally reduced by 1.0 to 0.94 in the optimized wing, implying efficient load alleviation. On the other hand, passive twist response experienced a remarkable increase in the optimized wing configuration by rising to 1.0 from 0.27, thereby proving the effectiveness of laminate tailoring in optimizing passive morphing capabilities. Moreover, weight reduction is evident as the normalized structural mass was normalized to approximately 0.71 in the optimized wing, which represents 29% of the structural mass. Hence, it is clear that the ANN-assisted NSGA-II optimization tool effectively optimized both conflicting aerodynamic and structural objectives.

Figure 15 shows the training performance of the neural network-based surrogate model used in the aero-structural optimization process. As indicated in the figure, the mean squared error (MSE) decreases rapidly during the early stages of the training process, reflecting effective learning of the aero-response surface and structural surface relationships. The training error (blue line) continues to decrease, reaching a very low level

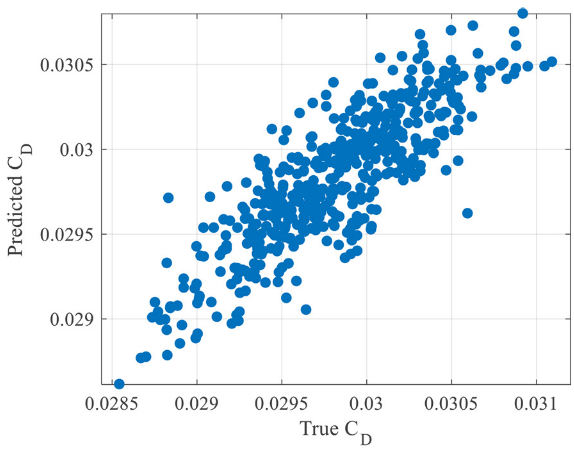

Figure 13. Predicted drag coefficient vs. true drag coefficient

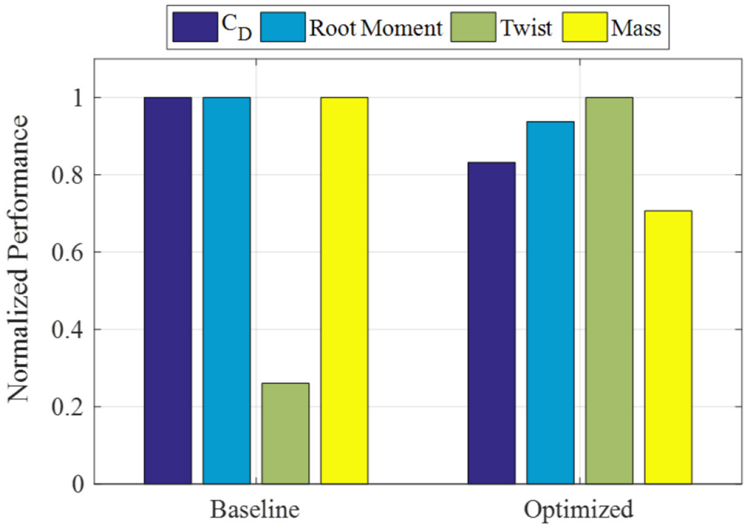

Figure 14. Baseline vs. optimization performance

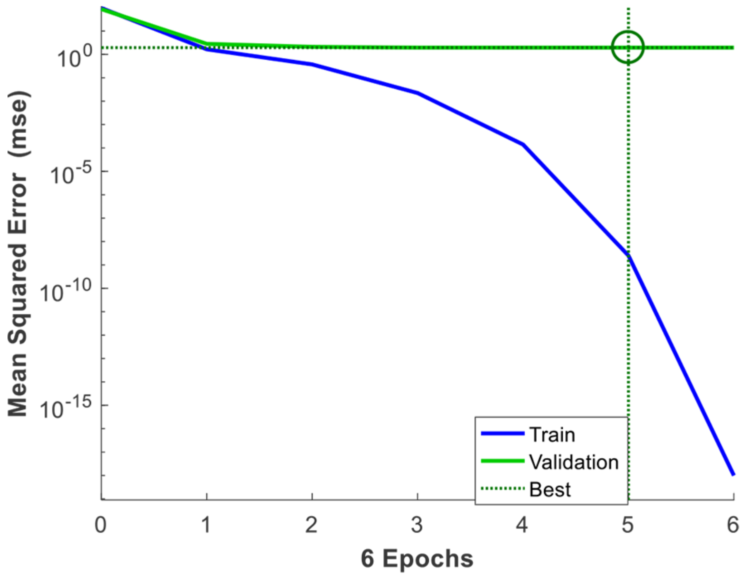

Figure 15. Best validation performance at epoch

after the sixth epoch. In contrast, validation error (green line) converges early in the training process, which indicates good generalization ability of the model. The best validation (dashed line) accuracy occurs at epoch 5, after which no further improvement is observed, indicating the effectiveness of the neural network model. The low validation error confirms the reliability of using the surrogate model in the optimization process.

CONCLUSIONS

The multi-objective optimization approach to passive morphing UAV wing design was successfully developed and validated. The surrogate model showed good predictive capabilities regarding aerodynamic and structural responses, with very close agreement between the predictions and reference values. The neural-network training process required a small number of epochs to converge, and the best validation result was obtained at epoch 5. This indicates the high generalization capability of the surrogate model. Optimization outcomes indicated a reasonable balance between aerodynamic efficiency, structural mass, and root bending moments. The optimal designs were found in a rather narrow design space with drag coefficient varying from 0.028 to 0.03, structural mass from 4.1 to 4.5 kg, root bending moment from 226 to 267 N·m, and passive twist angle from 2° to 8°. This means that passive aeroelastic tailoring of laminate optimization is an effective way to improve aerodynamics while preserving the structural efficiency and lightweight character. Moreover, the ANN-based NSGA-II optimization technique is computationally efficient and well-suited for tackling complicated aero-structural optimization tasks related to morphing UAV wings.

Further studies may include integrating the existing reduced-order model with high-fidelity computational fluid dynamics (CFD) and finite element analysis (FEA). Experimental work using composite morphing wings with corrugations could be carried out to confirm the aeroelastic behavior and vortex formation as predicted by the model. Moreover, future research may consider incorporating the effects of fluid-structure interaction, adaptive smart materials, and real-time control systems to enhance the aerodynamic performance of the next-generation UAVs design.

REFERENCES

1. Caixeta, P.R., Marques, F.D. Multiobjective optimization of an aircraft wing design with respect to structural and aeroelastic characteristics using neural network metamodel, Journal of the Brazilian Society of Mechanical Sciences and Engineering, 2018. https://doi.org/10.1007/s40430-017-0958-7
2. Grapin, R., Diouane, Y., Morlier, J. Regularized infill criteria for multi-objective Bayesian optimization with application to aircraft design, 2025; arXiv:2504.08671.
3. Ali Almutairi, M. A., Dunning, P., Maheri, A. Optimizing UAV winglets: A multiobjective approach with surrogate models, ECCOMAS Thematic Conference on MDO of Aerospace Systems, 2025.
4. Nikolaou, E., Kilimtzidis, S., Kostopoulos, V. Multi-fidelity surrogate-assisted aerodynamic optimization of aircraft wings, Aerospace 2025. https://doi.org/10.3390/aerospace12040359
5. İnci, H., Kayran, A. Surrogate model based optimization of variable stiffness composite wingbox for improved buckling load with manufacturing and failure constraints, Composite Structures, 2025. https://doi.org/10.1016/j.compstruct.2024.118571
6. Abbas, A.S., Mohammed, A.A. Experimental evaluation of morphing wing technologies: a systematic review, Revue des composites et des matériaux avancés 2025; 35(6): 1199–1209.
7. Liu, Y., Date, S., Nagashima, T., Okabe, T., Abe, Y. Effects of aeroelastic coupling accuracy and geometrical nonlinearity on performances of optimized composite wings, Aerospace Science and Technology, 2024. https://doi.org/10.1016/j.ast.2024.109926
8. Claret, R.B., Coelho, L., Fagiano, C., Julien, C., Lucor, D., Fabbiane, N. Reliability based optimisation of composite plates under aeroelastic constraints via adapted surrogate modelling and genetic algorithms, Composite Structures, 2024. https://doi.org/10.1016/j.compstruct.2024.118461
9. Moustapha, M. Multi-objective robust optimization using adaptive surrogate models for mixed parameters, 2022; arXiv:2203.01996.
10. Høghøj, L.C., Conlan-Smith, C., Sigmund, O., Andreasen, C.S. Simultaneous shape and topology optimization of wings, 2022; arXiv:2209.09330.
11. Miller, B., Ziemiański, L. Multi-objective optimization of thin-walled composite axisymmetric structures using neural surrogate models and genetic algorithms, Materials MDPI, 2023. https://doi.org/10.3390/ma16206794
12. Deb, K., Pratap, A., Agarwal, S., Meyarivan, T. A fast and elitist multiobjective genetic algorithm: NSGA-II, IEEE Transactions on Evolutionary Computation, 2002. https://doi.org/10.1109/4235.996017
13. Forrester, A.I.J., Sobester, A., Keane, A.J. engineering design via surrogate modelling: a practical guide, Wiley, 2008.
14. Horn, J., Nafpliotis, N., Goldberg, D.E. Multiobjective optimization using the niched Pareto genetic algorithm, Evolutionary Computation, 1994. https://doi.org/10.1162/evco.1994.2.2.73
15. Haftka, R.T., Gürdal, Z. Elements of Structural Optimization, 3rd Ed., Springer, 2012.
16. Friswell, M.I., Penny, J.E.T., Aeroelasticity of wing structures, Journal of Aircraft, 1985. https://doi.org/10.2514/3.48836
17. Hodges, D.H., Pierce, G.A. Introduction to Structural Dynamics and Aeroelasticity, Cambridge University Press, 2011.